Supporting information

8.0% Efficient Sub-Micron $CuIn(S,Se)_2$ Solar Cells on $Sn:In_2O_3$ Back Contact via a Facile Solution Process

Yao Gao[a], Guanchao Yin[b*], Yong Li[a], Tristan Köhler[a], Jan Lucaßen[a], Martina Schmid[a*]

[a] University of Duisburg-Essen, Faculty of Physics & CENIDE, Forsthausweg 2, 47057 Duisburg, Germany

[b] School of Materials Science and Engineering, Wuhan University of Technology, Luoshi Road 122, 430070 Wuhan, China

*Corresponding author: guanchao.yin@whut.edu.cn (Guanchao Yin)

martina.schmid@uni-due.de (Martina Schmid)

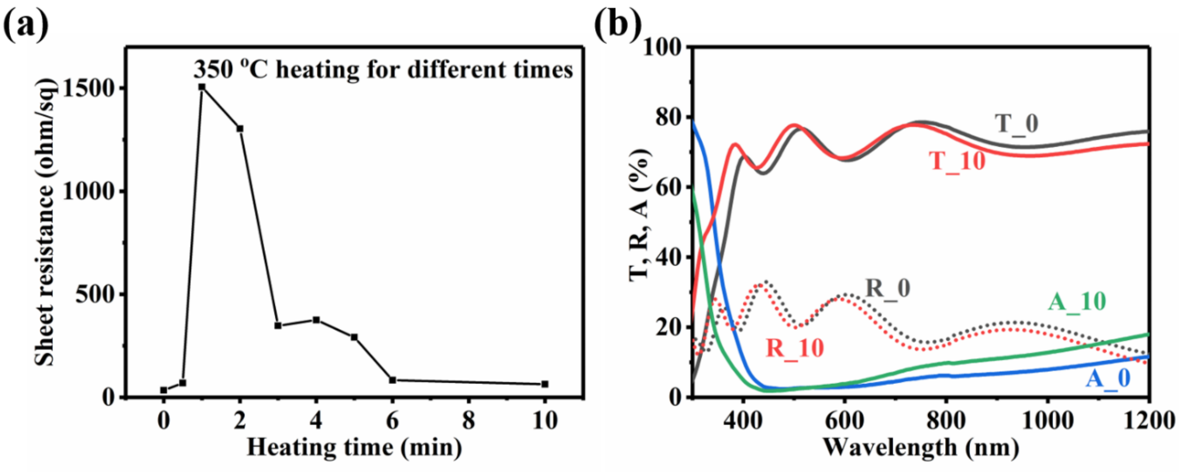

Figure S1 (a) Sheet resistance of 400 nm ITO films heated for different times at 350 ℃ under atmospheric conditions; (b) transmission, reflection, and absorption properties of 400 nm ITO without heating (T_0, R_0, and A_0) and with 10 min heating (T_10, R_10, and A_10).

Table S1 Composition of ultra-thin absorbers obtained under different selenization temperatures measured by XRF.

	Cu (at%)	In (at%)	Se (at%)	S (at%)	Cu/In	S/(S+Se)
500 ℃	21.63	28.52	47.36	2.12	0.76	0.04
520 ℃	19.50	25.32	35.23	19.62	0.77	0.36
540 ℃	20.60	26.08	39.74	13.19	0.79	0.25
560 ℃	18.04	23.83	25.86	31.92	0.76	0.55

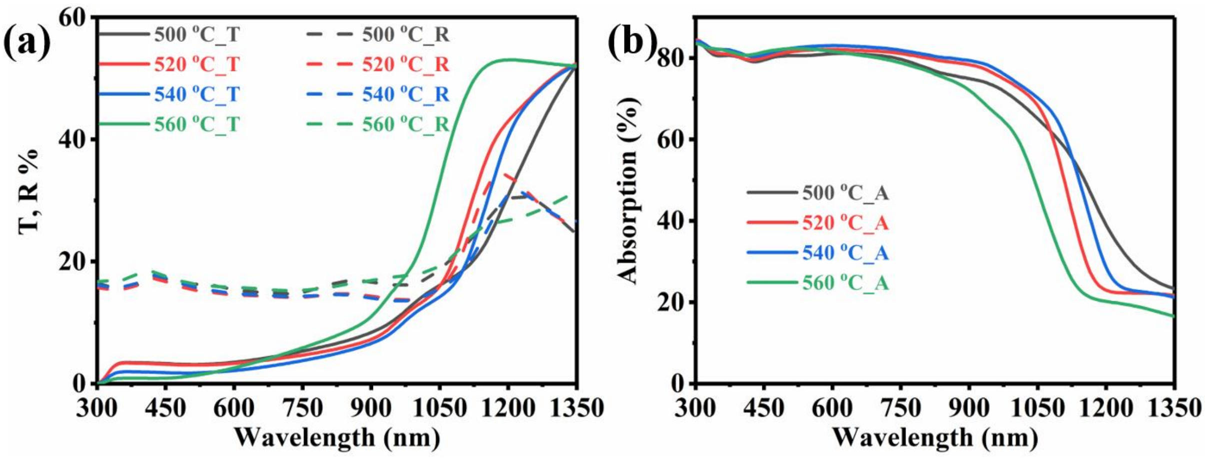

Figure S2 (a) transmission (solid line) and reflection (dashed line), (b) absorption of CISSe absorbers deposited on soda lime glass with various selenization temperatures.

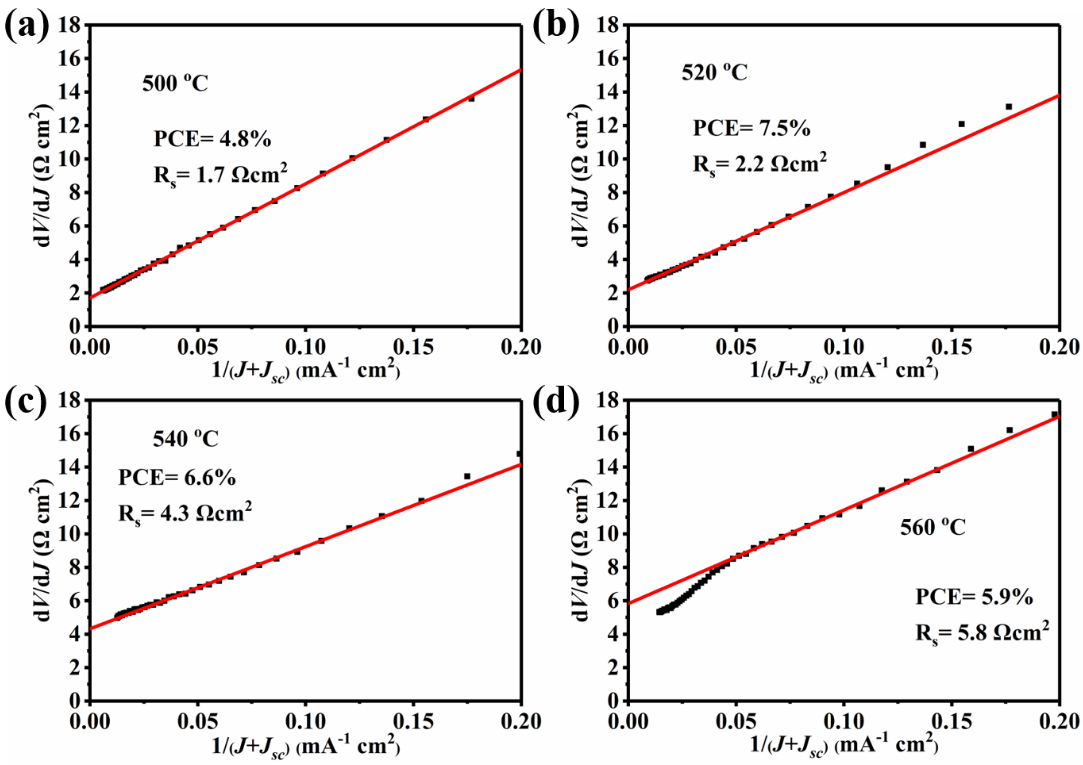

Figure S3 Determination of series resistance (R_s) for ultra-thin absorbers deposited on ITO back contact and selenized at different temperatures.

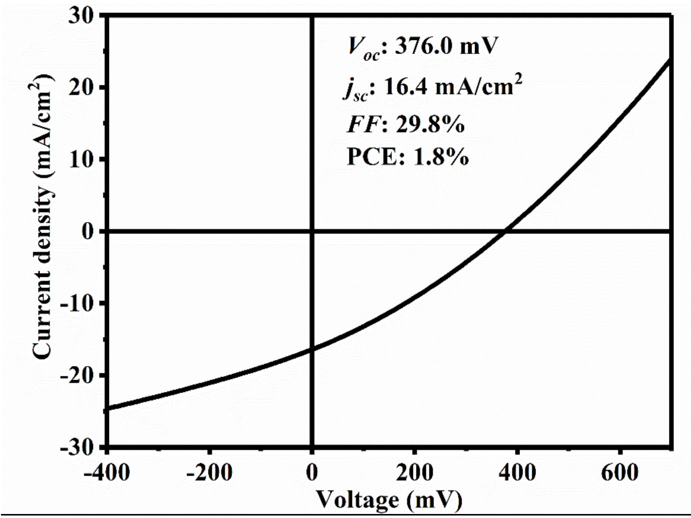

Figure S4 J-V curve of CISSe device with micron absorber thickness (1440 nm).

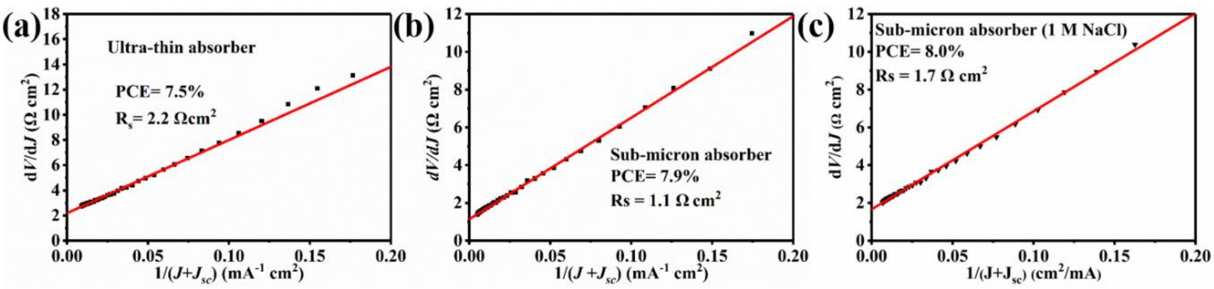

Figure S5 Determination of series resistance (R_s) for (a) ultra-thin absorber, (b) sub-micron absorber, and (c) sub-micron absorber with NaCl treatment deposited on ITO back contact and selenized at 520 °C.

Table S2 Averaged (over six devices) and best CISSe photovoltaic device parameters without and with various concentrations of NaCl treatment. The absorber thickness is 740 nm.

	V_{oc} (mV)	j_{sc} (mA/cm^2)	FF (%)	η (%)
no additional NaCl	448.5±2.6	29.1±0.6	56.3±3.2	7.3±0.4
	445.6	29.7	59.8	7.9
0.4 M NaCl	449.3±3.9	29.2±0.6	57.2±1.3	7.5±0.1
	450.0	29.2	58.8	7.7
0.8 M NaCl	432.6±9.9	28.3±1.2	53.4±3.3	6.5±0.6
	439.9	27.6	59.0	7.2
1 M NaCl	463.9±5.9	28.2±0.6	58.0±2.0	7.6±0.3
	466.0	28.7	59.6	8.0

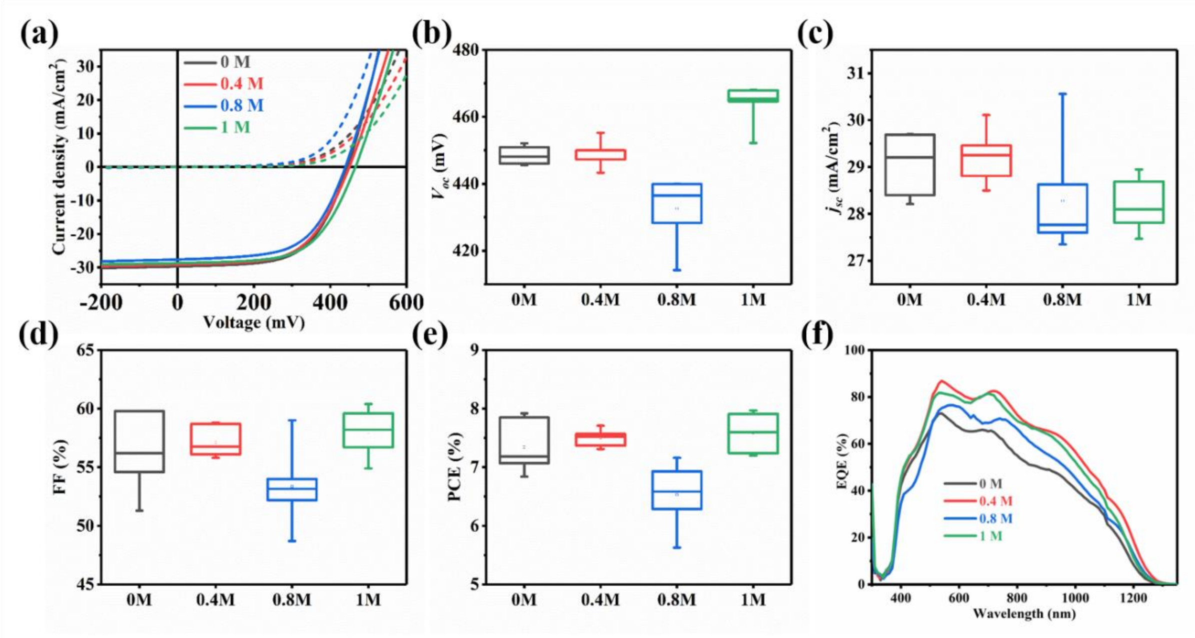

Figure S6 (a) *J*-*V* curves and (f) EQE spectra of the best sub-micron CISSe devices without and with different concentrations of NaCl for preselenization treatment. The distribution of (b) V_{oc}, (c) j_{sc}, (d) *FF*, and (e) PCE.

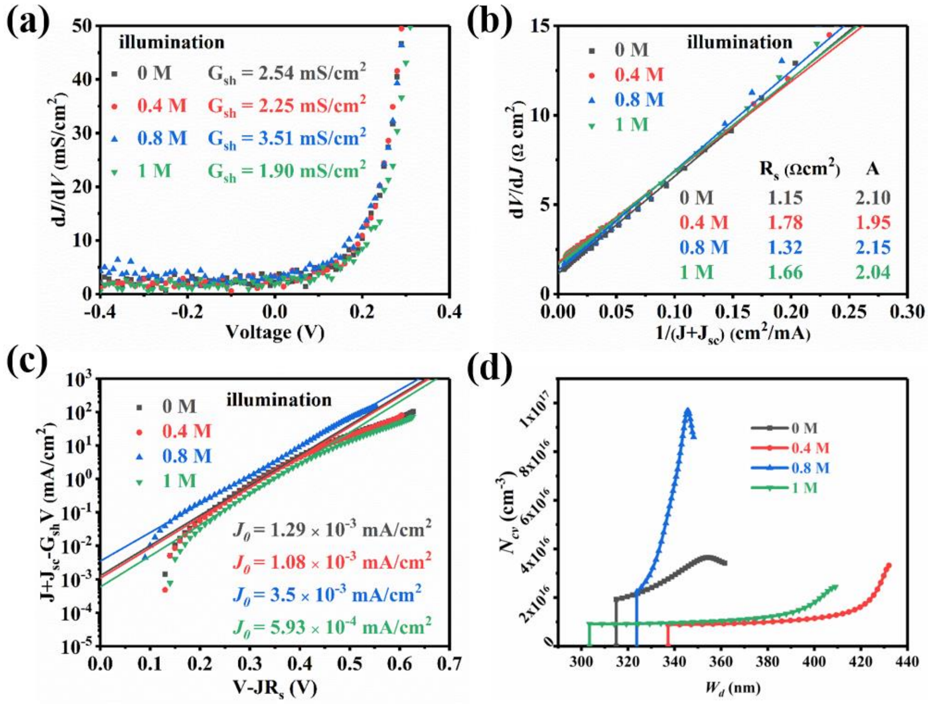

Figure S7 Plots of (a) d*J*/d*V* *vs.* *V* for extraction of G_{sh}, (b) d*V*/d*J* *vs.* $1/(J+J_{sc})$ for derivation of R_s and *A*, and (c) semi-logarithmic plot of $J+J_{sc}-G_{sh}V$ *vs.* $V-JR_s$ to determine J_0; (d) space-charge density N_{cv} and depletion width W_d for CISSe solar cells with sub-micron absorber without NaCl and with various concentrations of NaCl for preselenization treatment.

Table S3 Summary of electrical parameters extracted from further *J*-*V* and *C*-*V* analysis of the best CISSe solar cells without and with various concentrations of NaCl treatment. The absorber thickness was 740 nm.

	G_{sh} (mS/cm^2)	R_{sh} (Ω·cm^2)	R_s (Ω·cm^2)	j_0 (mA/cm^2)	A	N_{cv} (cm^{-3})	W_d (nm)
no additional NaCl	2.54	393.70	1.15	1.29×10^{-3}	2.10	1.9×10^{16}	315.0
0.4 M NaCl	2.25	444.44	1.78	1.08×10^{-3}	1.95	8.9×10^{15}	337.3
0.8 M NaCl	3.51	284.90	1.32	3.50×10^{-3}	2.15	2.2×10^{16}	323.8
1 M NaCl	1.90	526.32	1.66	5.93×10^{-4}	2.04	9.1×10^{15}	303.5

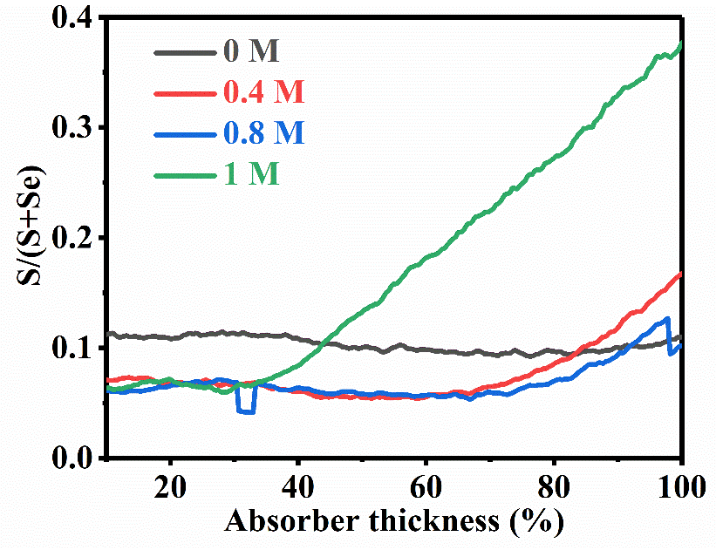

Figure S8 S/(S+Se) ratios of sub-micron absorbers subject to different concentrations of NaCl solution for preselenization treatment.

Table S4 Overview on high-performance CIGSSe-based solar cells deposited on transparent conductive back contact via a solution process.

Precursor	Deposition	Device	Thickness	η	Reference
Cu and In oxide NPs and Ga oxide	**Screen printing**	**FTO/Cu(In,Ga)Se_2/CdS/i-ZnO/ZnO:Al**	**1.3 μm**	**6.1%**	**[S1]**
$CuIn_xGa_{1-x}S_2$ nanoparticles	**doctor blading**	**FTO/Cu(In,Ga)Se_2/CdS/i-ZnO/ZnO:Al**	**2 μm**	**6.5%**	**[S2]**
$Cu(NO_3)_2$, $In(NO_3)_3$ and $Ga(NO_3)_3$	**spin-coating**	**ITO/Cu(In,Ga)S_2/CdS/i-ZnO/ZnO:Al**	**800 nm** **1.1 μm**	**5.7%** **6.6%**	**[S3]** **[S4]**
CuCl, $InCl_3$ and Thiourea	**spin-coating**	**ITO/CuIn(S,Se)$_2$/CdS/i-ZnO/ZnO:Al**	**550 nm** **740 nm**	**7.5%** **8.0%**	**Our work**

References

[S1] Sousa, V.; Goncalves, B. F.; Rosen, Y. S.; Virtuoso, J.; Anacleto, P.; Cerqueira, M. F.; Modin, E.; Alpuim, P.; Lebedev, O. I.; Magdassi, S.; Sadewasser, S.; Kolen'ko, Y. V. Over 6% Efficient Cu(In,Ga)Se_2 Solar Cell Screen-Printed from Oxides on Fluorine-Doped Tin Oxide. *ACS Appl. Energy Mater.* 2020, 3, 3120-3126.

[S2] Park, S. J.; Cho, J. W.; Park, G. S.; Jeong, J. S.; Kim, J.; Ko. D.-H.; Hwang, Y. J.; Min, B. K. A Comparative Study of Nanoparticle‐Ink‐Based CIGSSe Thin Film Solar Cells on Different Back Contact Substrates. *Bull. Kor. Chem. Soc.* 2016, 37, 361-365.

[S3] Barange, N.; Chu, V. B.; Nam, M.; Ahn, I. H.; Kim, Y. D.; Han, I. K.; Min, B. K.; Ko, D. H. Ordered Nanoscale Heterojunction Architecture for Enhanced Solution-Based $CuInGaS_2$ Thin Film Solar Cell Performance. *Adv. Energy Mater.* 2016, 6, 1601114.

[S4] Chu, V. B.; Park, S. J.; Park, G. S.; Jeon, H. S.; Hwang, Y. J.; Min, B. K. Semi-transparent Thin Film Solar Cells by a Solution Process. *Korean J. Chem. Eng.* 2016, 33, 880-884.